Industry Science and Engineering Vol. 2 No. 1, 2025

Intelligent Tennis Ball Picking Robot Based on Visual Recognition

Jiaqing Huang*, Yinying Li, Shuo Feng, Ruixi Guo, Peihong Zheng
College of Electrical Engineering, Southwest Minzu University, Chengdu, Sichuan, China
**Corresponding Author.*

Abstract: Aiming at the problem that most of the time in tennis training is spent on picking up scattered tennis balls and cleaning the court, an intelligent tennis ball picking robot based on visual recognition is designed. In the tennis ball picking robot, the color contour recognition method is first introduced to realize the visual recognition technology, and then the robot's autonomous navigation and obstacle avoidance are realized through the sensor fusion SLAM (Simultaneous Location and Mapping) mapping technology. The tennis ball picking and storage are completed by using the functional features such as visual recognition, SLAM mapping and rotating picking mechanical structure, and then the fine dust on the court is adsorbed by the electrostatic dust collector. After testing the relevant mechanical structure design and software implementation results, the designed intelligent tennis ball picking robot can effectively identify, pick up and store tennis balls, and has a good dust removal effect. This intelligent automatic tennis ball picking robot can be used on the tennis court, thereby improving the picking efficiency, saving time and saving human resources.

Keywords: Multi-Sensor Fusion Algorithm; SLAM; OpenCV Algorithm; Color Contour Recognition Method

1. Introduction

In recent years, the sport of tennis has shown significant growth worldwide. The global tennis population has exceeded 87 million, with a compound annual growth rate of 4.2%, among which the expansion of the Chinese market is particularly prominent. [1] According to the latest data from the Chinese Tennis Association, there are currently about 30 million tennis enthusiasts in China, accounting for 25.3% of the global total, and the number is tending to be younger. Eye in the Sky Data shows that as of August 2024, there are nearly 5,000 tennis-related companies in China. Starting from 2023, the number of registered related companies began to increase year-on-year. This growth is not only due to the improvement of public health awareness, but also benefits from national policy support for the sports industry (such as the "National Fitness Plan (2021-2025)") and the promotion of the commercialization of professional events (such as the Shanghai Masters, with an average annual increase of 12% in the number of spectators). However, problems such as low training efficiency and extensive field management are becoming increasingly prominent: traditional manual ball picking takes up 30%-40% of the total training time.

picking robot system that integrates intelligent ball picking and field cleaning. Compared with the ball picking robot that uses a drum-type ball collecting structure [2], the robot studied in this project uses a ball basket to store tennis balls. After completing the ball collecting work, there is no need to disassemble the ball collecting device to take out the tennis balls, which is more convenient and time-saving, and meets the goal of improving the efficiency of tennis training. The ball collecting device of the existing ball picking robot TennitBot on the market only allows one tennis ball to pass through at a time. In actual use, there are problems such as low ball collecting efficiency and overflow of pre-picked tennis balls. The ball picking structure equipped with the robot in this project can allow 3 tennis balls to pass through at a time. It has a simple structure, lower price and higher efficiency. Its task is to reduce the cost of intelligent equipment and reduce labor.

2. Robot Design

2.1 Overall Plan

The overall design of the robot is shown in Figure 1. It is divided into an upper computer and a lower computer. The upper computer is mainly responsible for identifying tennis balls, processing the identification information and transmitting instructions to the lower computer through serial communication. The lower computer is mainly responsible for controlling the chassis movement and dust removal function of the robot. At the same time, after receiving the instructions transmitted by the upper computer, it combines the feedback of its own sensors to make a comprehensive judgment, adjust the chassis movement and complete the tennis ball picking work.

Because the host computer is responsible for image acquisition and processing, serial communication with the slave computer, etc., it requires good data processing capabilities. At the same time, Python is selected as the programming language, which is simple and easy to use. Therefore, the Raspberry Pi with low cost-effectiveness, rich IO ports, and good support for Python is selected as the host computer. The slave computer is responsible for controlling the chassis movement, tennis ball picking and dust cleaning functions, and also requires more interfaces, so STM32F103C8T6 is selected as the slave computer. The communication between the host computer and the slave computer is realized through serial communication.

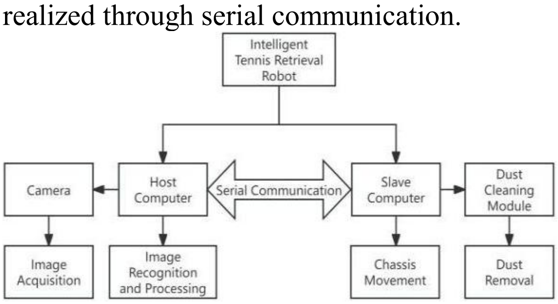

Figure 1. Overall Solution Diagram

2.2 Host Computer Selection

Since the robot needs high processing performance from the host computer for real-time processing after acquiring images through the camera, we chose the Raspberry Pi as the host computer, which has good general-purpose computer performance, strong storage capacity and data processing capabilities, and rich community resources. In addition, the Raspberry Pi system also comes with VNC software and Python, and the programming environment is more user-friendly and easy to use. At the same time, the flexibility and scalability of the Raspberry Pi facilitate the subsequent upgrade of the robot's functions.

2.3 Lower Computer Selection

The lower computer needs to control the chassis movement of the robot and the operation of the ball picking module and dust cleaning module, and at the same time needs to meet the serial port requirements for communication with the Raspberry Pi. Therefore, the lower computer uses STM32F103C8T6, which has the following advantages:

(1) It has rich peripherals, three communication serial ports, 64KB Flash + 20KB SRAM, and can make up for the storage limit through SPI;

(2) High cost performance, STM32F103C8T6 has 37 IO ports and 7 timers, 4 of which can be used to control the chassis and ball pickup module, and the operating frequency can reach up to 72MHz. It is cheap.

(3) Small package size, using LQFP48 package, small size and moderate pin spacing, the overall length of the MCU is 54mm and the width is 23mm;

(4) Low power consumption, with sleep, shutdown and standby modes. The operating current is 36mA at the highest main frequency and 2μA in standby mode. The core voltage is adjustable to further optimize power consumption.

2.4 Ball Pickup Module Design

The modeling of the ball picking module of this project is shown in Figure 2. It adopts a rotating leaf structure with an arc ④. Its movement is driven by two gears of the same model ②③ and a motor ①. Motor ① is interlocked with gear ②, gear ② is meshed with gear ③, and gear ③ is interlocked with the central axis of rotating leaf ④. When working, the lower computer controls the rotation of motor ①, and the torque is transmitted to rotating leaf ④ through the cooperation of various mechanical structures. Rotating leaf ④rotates counterclockwise, and the concave blades roll the tennis ball in. In order to prevent the tennis ball from flying and falling to the ground again when collecting the ball, a semicircular thin wall ⑤ is designed to prevent the flying phenomenon. The robot chassis and the ball picking module are interlocked through sheet metal ⑥⑦⑧. The diameter of the thin wall is 16cm, and the diameter of the tennis ball is between 6.54cm and 6.86cm, which will not affect the recovery of the tennis ball.

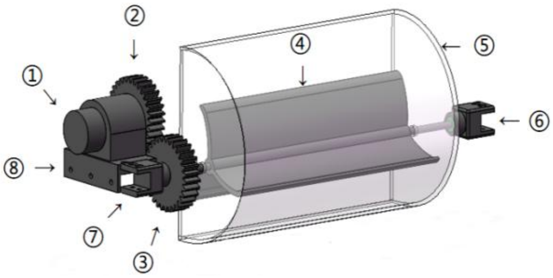

Figure 2. Solid Works Modeling Diagram of the Ball Picking Module

3. Robot Vision Processing

Current tennis ball collection devices face multiple technical challenges in practical applications. In terms of target recognition, although single tennis ball detection has high individual recognition accuracy, when multiple spheres appear in the visual acquisition area at the same time, the spatial overlap between the spheres will not only reduce the positioning accuracy but also cause data confusion problems. In terms of environmental adaptability, since the equipment is mostly operated in outdoor venues, the dynamic changes in sunlight intensity and incident angle will significantly change the light reflection characteristics of the sphere surface, thereby affecting the stability of visual features. In addition, the adhesion of surface contaminants caused by long-term use will form an optical interference layer on the surface of the sphere. This material degradation phenomenon will cause color distortion and texture feature attenuation, directly affecting the reliability of the recognition algorithm. To address the above technical bottlenecks, system performance can be improved through multi-dimensional optimization strategies, including using deep learning models to enhance target differentiation capabilities, building adaptive light compensation algorithms, and introducing multispectral imaging technology to penetrate surface pollution layers.

The project uses the HSV (Hue, Saturation, Value) color space theory to adjust and optimize images. The HSV color space can reflect the intuitive characteristics of color, also known as the hexagonal pyramid model. HSV conforms to human visual perception, and the use of the HSV color space is conducive to the project's setting of corresponding colors.

3.1 Color contour Recognition Method

The project uses color segmentation technology to extract the color features of the tennis ball to avoid the influence of factors such as light and shadow on visual recognition. [3] The digital images captured by the visual sensor use the red, green and blue three-primary color encoding system, and the color value of each pixel is represented by a three-element array. In order to realize the color gamut model conversion, the original color value components need to be normalized to the unit interval, and then the hue-saturation-brightness model is constructed through a specific mathematical relationship. The model contains three feature dimensions: the hue parameter is calibrated by circular angle, and the theoretical range covers 0-360 degrees of circular angle. However, due to the limitation of data storage format in the computer vision library, the actual range is compressed to half an angle, so the conversion result needs to perform a binary operation; the color purity parameter represents the degree of similarity between the color and the reference spectrum, and the brightness parameter reflects the optical energy intensity. The theoretical value range of both is a unit scalar, but in the image processing framework, in order to adapt to 8-bit integer storage, the calculation result needs to be linearly expanded by 255 times. It should be pointed out that the conversion process must strictly follow the numerical specifications of each development library to implement accuracy calibration.

The conversion formula from RGB (Red, Green, Blue) to HSV [4-7] is:

$$V = \max(R, G, B) \tag{1}$$

$$H = \begin{cases} 0(V - \min(R,G,B) = 0) \\ 60 \times \frac{G-B}{V-\min(R,G,B)}(V = R) \\ 60 \times \frac{B-R}{V-\min(R,G,B)} + 120(V = G) \\ 60 \times \frac{R-G}{V-\min(R,G,B)} + 240(V = B) \end{cases} \tag{2}$$

$$S = \begin{cases} \frac{V-\min(R,G,B)}{V}(V \neq 0) \\ 0(V = 0) \end{cases} \tag{3}$$

Figure 3. RGB Color Image of Tennis Ball

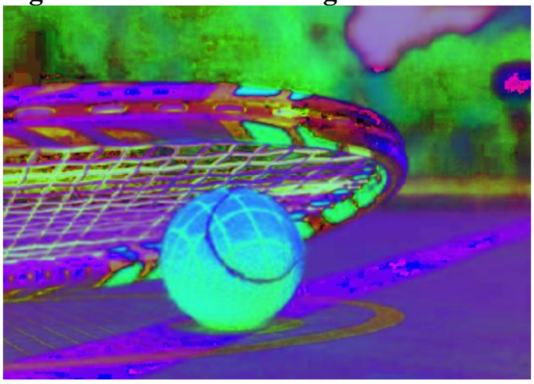

Figure 4. HSV Color Image of Tennis Ball

The specific steps of the tennis detection scheme are as follows: the system obtains the original image through the image sensor connected to the Raspberry Pi. After image optimization processing such as noise reduction and brightness adjustment, the OpenCV recognition algorithm is used to analyze the processed image features. When the algorithm determines that there is a target that meets the color characteristics of the tennis ball, the system will output a control signal to drive the mechanical device through the development board. The whole process uses a continuous polling mechanism to ensure real-time monitoring. Figure 3 shows the original image acquisition screen of the tennis court, which is processed by the color space conversion tool to generate an HSV color picture, as shown in Figure 4. The conversion process converts the image from the RGB three-color mode to the HSV color mode. In the converted image, the surface of the tennis ball shows an obvious yellow area (corresponding to the hue value range of 30-35 degrees), which provides a reliable basis for subsequent target positioning. Actual tests show that the use of hue feature analysis can effectively distinguish tennis balls from environmental backgrounds. Under typical outdoor lighting conditions, the recognition accuracy is greatly improved compared with traditional methods. The system achieves stable recognition of targets by establishing a color threshold model.

By converting the original captured image into HSV color space, the tennis ball is segmented, and the values of its hue, saturation, and brightness are observed to determine the value range of the target tennis ball as the segmentation connection. In order to further identify the features of the tennis ball, the inRange function is used to segment and binarize the tennis ball and the field background, as shown in Figure 5. It can be seen from the observation that after the binarized image is preprocessed and Gaussian filtered with a kernel of three, the outline of the target tennis ball is approximately circular. The contour search function findCountours in OpenCV is used and the EXTERNAL contour retrieval mode is set. This processing can ignore the internal contour of the target circle. Finally, the drawCountors function in OpenCV is used to mark the target tennis ball, so that the outline of the target tennis ball in the original image is framed by a rectangle, and the effect Figure 6 is output, which intuitively shows the position and shape of the tennis ball.

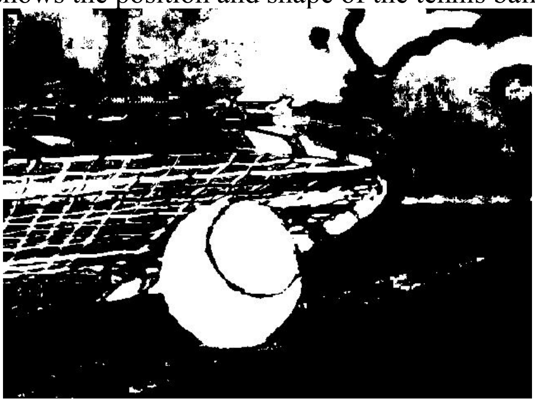

Figure 5. Binarized Tennis Ball Image

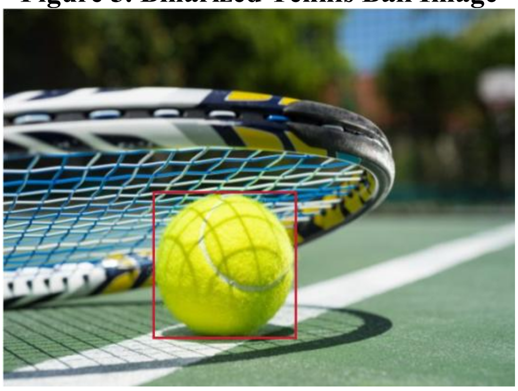

Figure 6. Effect of Color Contour Recognition Method

3.2 Multi-sensor Fusion Method

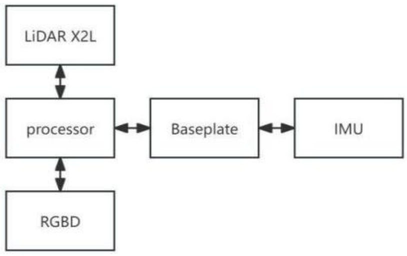

Figure 7. Platform Hardware Structure Framework

The project used the multi-sensor fusion technology Slam mapping method [8] to avoid the limitations of external perception when using a single sensor [9] and solved the problem of robots bumping into each other on the tennis court due to obstacles and tennis balls easily falling to the side of the court.

The robot is equipped with a laser radar and a visual sensor. The laser radar uses X2L, with a maximum measurement distance of 8m and a maximum frequency measurement distance of 3000Hz. The visual sensor uses RGBD, with a measurement range of 0.1m ~ 10m and a frequency of 30FPS. Raspberry Pi is selected as the processor. The chassis of the car uses the PI D differential control method to meet the real-time mapping and positioning navigation functions of the single-line laser radar fusion RGBD. Figure 7 shows the hardware structure framework of the platform. The perception sensors equipped on the robot are used to collect environmental information. When the robot moves, these sensors will transmit data information to the processor. Subsequently, the processor processes the data through an algorithm and finally generates the corresponding map and navigation positioning information.

The multi-sensor fusion algorithm used in the project adopts a post-fusion strategy. The specific block diagram is shown in Figure 8. After each sensor completes the detection and segmentation tasks, the data is fused. The timestamp data will be sent through the sensor in the prediction stage, and then spatial alignment will be performed according to the motion state. After the previous frame observation is associated with the current observation, the current frame state is estimated by combining the observation and state quantities, and the target-level and semantic-level driving phenomena can be obtained.

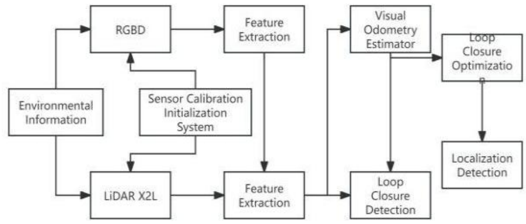

Figure 8. Fusion Algorithm Block Diagram

In the prediction problem, when the robot is driving during the sensor fusion process t, the state of the robot system is not updated in time and is still displayed as $\mathrm{t}-1$the state value at the moment $\mathrm{S}_{\mathrm{t}-1}$, but the sensor measurement value is M_{t} . In order to complete the time-space alignment, the robot's state value needs to be updated to S_{t}. Because the laser radar contains posture, velocity and acceleration information, the transformation matrix is used here to complete the synchronization of posture state and motion state. The alignment of the target level and the semantic level can be completed using formula (4):

$$S_t = P_t^{t-1} S_{t-1} \tag{4}$$

Where, $\mathrm{P}_{\mathrm{t}}^{\mathrm{t}-1}$ represents $\mathrm{t}-1$ the pose increment from time to time.t

For target-level motion attribute fusion, it is usually assumed that the target is rotating at a constant speed or moving in a straight line with uniform acceleration, and the target state transfer equation is:

$$x_t = \boldsymbol{F}_t x_{t-1} + \boldsymbol{B}_t u_t + \omega_t \tag{5}$$

In formula (**5**), $\mathrm{x}_{\mathrm{t}}$is the observed value of the target at time t; $\mathrm{F}_{\mathrm{t}}$is the state transfer matrix, which represents $\mathrm{t}-1$ the state change from B_{t}time t to time t, $\mathrm{t}$represents the conversion relationship matrix between the input of the tennis court and the state change of the visual system; u_{t}represents $\mathrm{t}$the input of the system at time t; ω_{t} is the system noise, which satisfies the Gaussian distribution and $\mathrm{N}(0,\mathrm{Q}_{\mathrm{t}})$, Q_{t}represents $\mathrm{t}$the variance at time t.

The project robot is an intelligent system that can autonomously complete the ball picking function. It belongs to a zero-input system and is solid u_{t} 0. Therefore, the original formula can be simplified to

$$x_t = \boldsymbol{F}_t x_{t-1} + \omega_t \tag{6}$$

For further comparison, this paper mainly conducts tests from the perspective of laser radar and RGBD visual sensor fusion mapping. The fusion modeling diagram is shown in Figure 9.

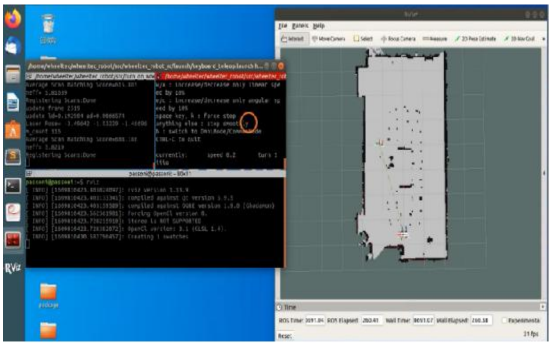

Figure 9. LiDAR and Visual Sensor Fusion Map Construction

During the test, the unmanned vehicle turned on the laser radar and RGBD camera, drove from the starting point to the obstacle box, and obtained the test results of sensor fusion mapping. At the same time, in the test scene, the unmanned vehicle cycled back and forth many times to obtain complete mapping test results. Since the entire mapping process integrates visual information, the constructed map is closer to the actual scene environment. After the mapping is completed, the map scene contains the three-dimensional detail information of the entire scene, providing more accurate information for subsequent navigation positioning and collision avoidance. When the laser radar and visual sensors turn on fusion mapping, a real-time obstacle detection perspective map can be obtained. When the unmanned vehicle approaches the obstacle box in the test scene, the visual depth map of the obstacle box can be detected; when the unmanned vehicle returns to the starting point during the mapping process, the visual depth map of the person and the plastic stool at the starting point of the test scene can be detected. From the test results, whether it is an obstacle in the test scene or an obstacle at the starting point, their height, volume, and three-dimensional shape details are finely reflected in the constructed map data, which is extremely critical for the real-time positioning and three-dimensional collision avoidance of the autonomous driving vehicle. During the sensor fusion mapping process, observe the CPU occupancy rate. Since the processor needs to process the data of the lidar and visual sensors at the same time, and the data volume of these two types of perception sensors is large, the processor occupancy rate is maintained at more than 40% during the entire operation, and the peak can reach about 45%. At this time, if the processor needs to perform other operations, the remaining processor resources will be relatively tight, and the processor may even crash and restart. When only lidar is used for mapping, the CPU occupancy rate is about 10%. Practical results have shown that the fusion of lidar and visual sensors performs well under good lighting conditions and is suitable for SLAM mapping of intelligent tennis ball picking robots.

4. Robot Motion Control

4.1 Hardware Selection

Robot chassis control is a key link in the intelligent robot system. Its main task is to achieve precise movement and stable operation of the robot. In the intelligent tennis ball picking robot, the design and implementation of the chassis control system is crucial to the overall performance of the robot. Here we review the basic principles, key technologies, system design and practical applications of robot chassis control and discuss the chassis control of the robot in this project.

The core of robot chassis control is to achieve robot motion control through the coordinated work of motor drive system, sensor feedback and control algorithm. The motor drive system is responsible for providing power, the sensor feedback system monitors the robot's motion state in real time, and the control algorithm adjusts the motor output according to the sensor feedback to achieve the expected motion trajectory and posture. The robot 's chassis control system adopts a differential control method to achieve the robot's steering and motion control by adjusting the speed difference between the left and right wheels. Specifically, by adjusting the speed of the left and right wheels, the robot can achieve basic movements such as forward, backward, and turning. As mentioned above, the chassis control system integrates path planning and obstacle avoidance functions. Through multi-sensor fusion technology, the robot can autonomously navigate and avoid obstacles in complex environments.

The chassis modeling of the robot is shown in Figure 10. As the hardware for controlling the movement of the chassis, the selection of motors and wheels is crucial. The robot's working environment is a tennis court, and a high-precision, high-torque, low-speed, and reliable motor is required to cooperate with the PID algorithm so that the robot can run at a constant speed during work to avoid accidental injuries to athletes. The wheels need to move omnidirectionally to track the tennis balls scattered on the tennis court. This project uses a 520 encoder DC reduction motor and a Mecanum wheel.

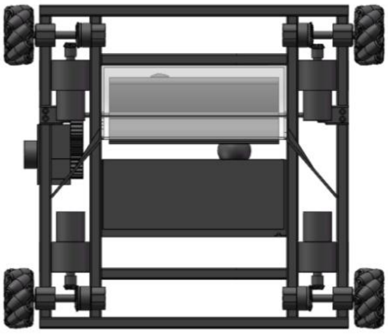

Figure 10. Robot Chassis Modeling Diagram

4.2 Control Methods

In terms of motor control algorithm, the most common controller PID (Proportional-Integral-Derivative Controller) control method is adopted, the core of which is proportion (K_P), integration (K_i)and differentiation (K_d). Its working principle is shown in Figure 11.

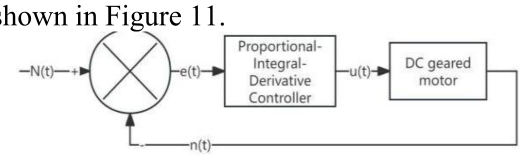

Figure 11. PID Control Principle Diagram

The target speed of the control system in the figure $N(t)$ is numerically compared $e(t) = n_0(t) - n(t)$ with the actual speed, and the error is obtained through calculation $n(t)$. After the speed error is optimized by the PID controller, its output voltage signal is u(t). This voltage signal is power-amplified and used to drive the DC motor, thereby adjusting the motor speed to reduce the speed error until the actual motor speed reaches or approaches the target speed.

PID control methods are mainly divided into incremental and position types. The incremental PID algorithm has the characteristics of simple program implementation, stable operation, and fast calculation speed. Therefore, the robot chassis control adopts the incremental PID algorithm [10,11]. Its principle formula is as follows:

$$u(k-1) = k_p\big(e(k-1) + k_i \textstyle\sum_{j=0}^{k-1} e(j) + k_d(e(k-1) - e(k-2))\big) \quad (7)$$

According to the principle formula, the incremental PID algorithm can be derived.

$$\Delta\, u(k) = \quad u(k) - u(k-1) \quad (8)$$

$$\Delta\, u(k) = k_p(e(k) - e(k-1)) + k_i e(k) + k_d(e(k) - 2e(k-1) + e(k-2)) \quad (9)$$

In the above formula, $e(k) - e(k-1)$ is the proportional term, which represents the difference between the current error and the last error, $e(k)$ is the integral term, which represents the current error, $e(k) - 2e(k-1) + e(k-2)$ and is the differential term, which represents the difference between the last proportional term and the current proportional term. From the incremental PID formula, it can be well seen that once k_p ,, k_i and are determined k_d , the control increment can be calculated by the formula by using the deviation of the three previous and subsequent measurement values $\Delta\, u(k)$. The obtained control increment corresponds to the increment of the position error in recent times, rather than the deviation from the actual position, and there is no error accumulation. In other words, no accumulation is required in the incremental PID. The determination of the control increment $\Delta u(k)$ is only related to the sampling values of the last three times, and it is easy to obtain a better control effect through weighted processing, and when problems occur in the system, the incremental type will not seriously affect the operation of the system.

5. Simulation Results Verification

According to the descriptions in the above chapters, SolidWorks was first used to create a three-dimensional model of the robot, as shown in Figure 12.

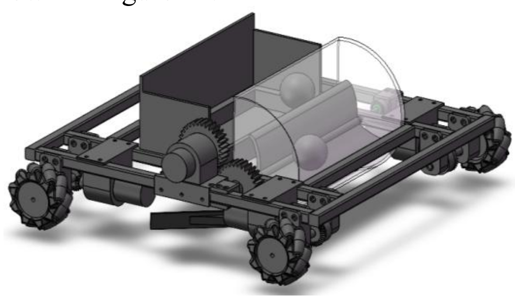

Figure 12. SolidWorks Modeling Diagram of the Intelligent Tennis Ball Picking Robot

To verify the practicality of the modeling, it was imported into SolidWorks Simulation to perform simulation analysis on the robot's mechanical structure, kinematics, dynamics, and control algorithm.

After importing the model, input the robot's physical parameters, such as mass, center of mass position, moment of inertia, wheel radius, motor parameters, friction coefficient, etc., which will directly affect the parameters of the simulation results. Then set the initial conditions of the simulation, such as the robot's initial position, speed, posture, etc., as well as external environmental conditions, such as ground friction coefficient, slope, etc. Since the robot's work site in this project is a tennis court, the fixed slope is 0. Finally, it is necessary to set the proportional coefficient, integral coefficient, differential coefficient, etc. of the control algorithm in the simulation, and adjust and optimize as needed.

After simulation experiments, the robot demonstrated stability and safety under different basic parameters and initial conditions. Based on the control of the PID algorithm and the visual recognition of the multi-sensor fusion algorithm, the robot can flexibly avoid obstacles and complete the ball picking task at a high initial speed.

6. Conclusion

In summary, the intelligent tennis ball picking robot based on visual recognition designed in this study shows good performance and application potential in tennis ball picking and court cleaning. By introducing advanced convolutional neural networks, YOLO models, and SLAM mapping technology, combined with a carefully designed mechanical structure and motion control system, the robot can efficiently identify and pick up tennis balls and clean the court, effectively solving problems such as time-consuming manual ball picking and extensive court management in traditional tennis training, significantly improving training efficiency and saving time and human resources.

In future practical applications, this intelligent tennis ball picking robot is expected to be widely promoted in various tennis venues, providing strong support for the development of tennis. At the same time, with the continuous advancement and innovation of technology, we will continue to optimize and improve the robot to further enhance its performance and functions, such as optimizing the visual recognition algorithm to improve the recognition accuracy in complex environments, improving the motion control system to achieve more precise motion control, and exploring more intelligent functional modules to better meet the needs of tennis training and venue management, and contribute more to the intelligent development of tennis.

Acknowledgments

This paper was supported by Student innovation and entrepreneurship training program of Southwest Minzu University (D202411151609013460).

References

[1] Chang Li. Tennis is heating up. Economic Daily, 2024-10-28(010). DOI:10. 28425/n.cnki.njjrb.2024.007529.
[2] Deng Shichun, Pan Jiasong, Deng Jun, et al. Automatic tennis ball picking robot based on Raspberry Pi and OpenCV vision technology. Mechanical and Electrical Engineering Technology, 2024, 53(07): 60-63.
[3] Wang Yuguan, Zhong Peng, Zheng Guibin, et al. Application of YOLOv5 in tennis ball recognition. China Science and Technology Information, 2023, (19): 115-119.
[4] Zhang Xuexi, Yang Yimin. Commonly used color spaces and their conversion in color image engineering. Computer Engineering and Design, 2008, (05): 1210-1212. DOI: 10.16208/j. issn1000-7024.2008.05.041.
[5] KRUSE, ANDREW W., ALENIN, ANDREY S., VAUGHN, ISRAEL J., et al. Perceptually uniform color space for visualizing trivariate linear polarization imaging data. Optics Letters, 2018,43(11):2426-2429. DOI:10.1364/OL.43.002426.
[6] YIN, WEI, CHENG, XIAOSHENG, CUI, HAIHUA, et al. Adaptive and accurate color edge extraction method for one-shot shape acquisition. Optical Engineering, 2016,55(9):094104-1-094104-11. DOI:10.1117/1.OE.55.9.094104.
[7] VERMA, OM PRAKASH, PARIHAR, ANIL SINGH. An Optimal Fuzzy System for Edge Detection in Color Images Using Bacterial Foraging Algorithm. IEEE Transactions on Fuzzy Systems: A Publication of the IEEE Neural Networks Council,2017,25(2):114-127.

DOI:10.1109/TFUZZ.2016.2551289.

[8] Ma Zhiyi. Research on autonomous navigation system based on multi-sensor fusion SLAM. Shaanxi: Chang'an University, 2023.

[9] A review: On path planning strategies for navigation of mobile robot. Defense Technology, 2019, 15(4): 582-606. DOI: 10.3969/j.issn.2214-9147.2019.04.014.

[10]Zhao Gaochao, Yang Hongwu, Pei Dong, et al. Motor incremental PID control system based on TMS320F2812. Instrument Technology and Sensor, 2014(6):106-108,112. DOI: 10.3969/ j. issn.1002-1841.2014.06.033.

[11]Zhu Rongtao, Wu Hongtao. DC motor speed control system based on incremental PID algorithm. Instrument Technology and Sensor, 2017(7):121-126. DOI: 10. 3969/j.issn.1002-1841.2017.07.031.